ASIAN JOURNAL OF CIVIL ENGINEERING (BHRC) VOL. 17, NO. 1 (2016)
PAGES 15-42

INVESTIGATION OF THE EFFECTIVE PARAMETERS ON THE STRENGTH AND DUCTILITY OF THE WELDED FLANGE PLATE CONNECTIONS

A.A. Hedayat[1*] , H.Saffari[2] and E. Jazebi[1]
[1]Civil Engineering Department, Kerman-branch, Islamic Azad University, Joopar road, Kerman, Iran
[2]Civil Engineering Department, Shahid Bahonar University of Kerman, Kerman, Iran

Received: 15 June 2015; **Accepted:** 12 August 2015

ABSTRACT

After Northridge earthquake several connection configurations have been proposed by researchers to improve the ductility of the rigid connections. One of them is welded flange plate (WFP) connections. These connections have been used in Iran for years but with different details from what is presented by the Federal Emergency Management Agency (FEMA). In present study a parametric study on the strength and ductility of WFP connections in the case of utilizing deep beams has been carried out using finite element method. These parameters are; beam material property, flange plate thickness, flange plate length, the transverse welding of the top flange plates, the end form of the top flange plate, the equality or inequality of the top and bottom flange plate length, form of the rib plates and the common methods to transfer the shear force from the beam to the column. Finally, the effects of doubler plates to increase the strength and ductility of the WFP connections were investigated.

Keywords: Special moment frame; ductility; strength; welded flange plate (WFP) connection.

1. INTRODUCTION

The steel moment-resisting frames suffered a verity of brittle fractures in their beam-to-column connections during the 1994 Northridge earthquake. This initiated widespread research to find out the causes [1-3] and to propose changes to design procedures. Several methods have been presented so far in order to increase the ductility of pre-Northridge connections. These modifications can be implemented either by reinforcing the connection or weakening the beam section. The purpose of each method is to create a stronger

*E-mail address of the corresponding author: amirahmad1356@yahoo.com (A.A. Hedayat)

connection in comparison with the beam. Using these methods lead to move the plastic hinges in a region away from the face of the column and avoid the brittle fractures. In the first method some additional elements are added to the connection at the column face level [4-6], while in the second method, weakening the beam section can be done either by cutting a portion of the beam flange, (reduced beam section connections, [7]) or the beam web (RBW connections,[8-11]).One of the most common used methods after Northridge earthquake to enhance the ductility of rigid connections was using plates in two forms of cover plate and flange plate (Fig. 1). The latter is named by FEMA350 (2000) [12] as welded flange plate (WFP) connection where the width and the length of the top flange plate are as same as those of the bottom flange plate.

Prior to the Northridge earthquake, a number of investigators conducted cyclic loading tests on steel moment connections reinforced with cover plates [13]. These early tests showed that very high levels of cyclic ductility could be achieved by reinforced connections. However, these earlier tests were very limited in number and were conducted on relatively small size of beams. Popov and Jokerst[14] tested two WFP connections which were composed of W30x99 beams and W14x283 columns of ASTM A572 Grade 50 steel. Two connections were reinforced by two same size and trapezoidal shaped flange plates. Both specimens achieved 0.034 radian plastic rotations. Whittaker and Gilani [15] tested three WFP connections. Specimens were composed of W21 and W24 beams and I-shaped columns of Grade 50 steel with two same size-rectangular shaped flange plates. They investigated the effect of contribution of the column panel zone (PZ) to the plastic rotation capacity of the joint. In these tests, in the case of having weak PZ, the large distortions in the PZ led to the column flange fracture and caused minimum contribution of the beam into the joint plastic rotation capacity. The joint plastic rotation capacity varied between 0.028 and 0.045 radian. All specimens (except the specimen of weak PZ) experienced excessive strength degradation. Noel and Uang [16] tested three double-sided and one single-sided WFP connections. The beams ranged from W24x94 through W18x86 of Grade 50 steel with two same size rectangular or trapezoidal shaped flange plates. Maximum beam plastic rotation ranged between 0.013 and 0.046 radian. A total of 12 large scale specimens were constructed with cover plated connections and subjected to cyclic loading tests by Engelhardt [4]. Out of the 12 specimens tested by Engelhardt et al. [4], 10 specimens showed excellent performance, achieving high levels of plastic rotation. Tests done by Engelhardt et al. [4] indicated that using very long cover plates could result in a large amplification of moment from the hinge location to the face of the column. This research also showed that using very thick cover plates result in a very high restraint at the face of the column, thereby promoting more brittle behavior.SAC Joint Venture (SAC 2000) [17] tested five WFP and five cover plate reinforced connections. All specimens were fabricated from W30x99 Grade 50 beams and Grade 50 rectangular or trapezoidal shaped reinforcing plates. The key design variables were loading history, PZ strength and stiffness (which several investigation on the behavior of panel zone have been done [18-20]), and flange plate thickness and geometry. The results revealed substantially better behavior in these types of connections as opposed to unreinforced connections. None of the ten connections failed in a brittle manner and the maximum beam plastic hinge rotations ranged between 2.3% and 3.9% radians. However, specimens experienced excessive strength degradation at large rotations.

WFP connection is also the most common connection in Iran while its configuration and fabricating processes is different from what has been mentioned in FEMA350 (2000) [12] and this may lead to the achievement of a different behavior. Fig. 2 shows this connection where the bottom beam flange has been strengthened by using a rectangular flange plate which is wider than the beam flange. Whilst, the top beam flange has been strengthened by using a flange plate which is narrower than the beam flange. In this connection, the bottom flange plate is shop welded to the column flange which is consequently used as a seat plate during the erection process of the structure. Whilst the top flange plate is field welded to the column flange. These forms of plates prevent overhead welding which finally leads to the achievement of a stronger weld. Ghobadi et al. [21] [22] and Gholami et al. [23] tested few WFP connections where the connection configuration was similar to what is common in Iran (i.e. similar to Fig. 2). In all tests the section used for beams was either IPE270 (beam depth=270 mm) or a built up section with the overall depth equal to 380 mm. The key design parameters in these tests were: (1) type of weld for connecting the bottom beam flange plate to the column flange, (2) T-stiffeners for retrofitting purposes, (3) flange plate length, and (4) plate-to-beam flange fillet weld geometry. Based on the experimental tests done by Gholami et al. [23] and Ghobadi et al. [10], the WFP connections used in Iran can reach to an acceptable level of ductility. It should be noted that in these tests, the maximum beam depth was only 380 mm. However, such beams are generally referred as shallow beams. Shallow beam connections often show a high plastic rotational capacity even in the case of using pre-Northridge connections (FEMA355D, 2000) [24]. Because of this, generally all connection modifications are developed by using deep beams (e.g. W36x150, W30x99 and W24x68 beams). In addition, for all specimens tested by Gholami et al. [23] and Ghobadi et al. [21]a single shear tab was used to transfer shear force from the beam to the column. While, in Iran, in order to transfer the shear forces, normally the rib plates are used. All these differences finally may lead to the achievement of different behavior from that has been mentioned by the FEMA350 [12] or Gholami et al. [23] and Ghobadi et al. [21].

Hence, the present study was aimed to do a parametric study on the behavior of WFP connections by using deep beams considering all mentioned details used in Iran to reach a better understanding of the behavior of such connections. The key design variables were: flange plate thickness, methods to transfer shear force from the beam to the column, transverse welding at the noise of flange plates, end form of the top flange plate, equality and inequality of the top and the bottom plate length and rib plate form. Most of these parameters were not investigated by previous researchers. In addition, experimental tests done by SAC2000 [17] and Whittaker and Gilani [15]showed that in the case of using deep beams, the WFP connection experiences remarkable strength degradation such that at 4 percent total rotation the connection may not reach to 80% of the beam plastic moment capacity. However, such significant strength degradation was not reported by Gholami et al. [23] and Ghobadi et al. [21] where the shallow beams were used. Hence, the last aim of this study was to investigate the efficiency of doubler plates to resolve such problem for deep beams.

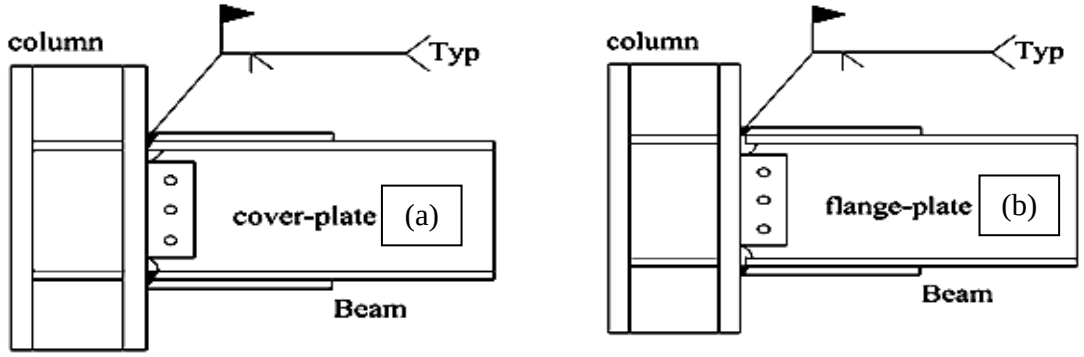

(a) Cover plate (b) Flange plate

Figure1. Using plates

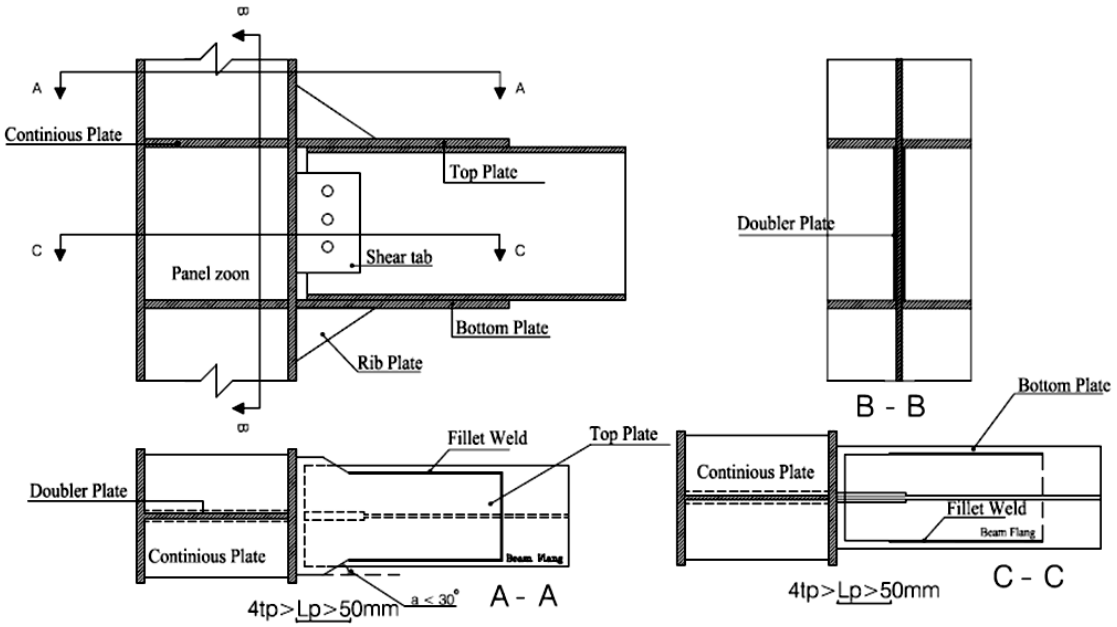

Figure 2. The common rigid connection (WFP connection) in Iran

2. FINITE ELEMENT MODELING

In order to verify the accuracy of finite element modeling, at first, specimens RC06 of reference (SAC2000) [17] which its configuration is based on the FEMA350 (2000) [12](i.e. rectangular flange plates) was remodeled using ANSYS software [25]. The used materials for both beam and column were made of A572 Grade 50 steel (SAC 2000)[17]. For this specimen the length of the column and the beam were 3450 mm and 3400 mm respectively. The thickness of the continuity plates and the web doubler plate are 25 mm and 10 mm respectively. The high fracture toughness weld metal used was E70. Fig. 3 shows the finite

element mesh of this specimen. In this model, all connection's parts were modeled using shell elements (SHELL181 in ANSYS program). Interaction between plates (e.g. interaction between the flanges of beam and the top or the bottom flange plates) was modeled using contact elements.SHELL181 is a multi-layer four-node shell element which has the ability to model plasticity, large deflection, and large strain phenomena. In this case each element was separated into five layers across the thickness. The number of layers was selected based on the finite element study carried by Gilton and Uang [26]. In order to determine the appropriate mesh density, a study on mesh sensitivity was carried based on the recommendations given by ANSYS software. Results were then compared with the experimental results presented by SAC (2000) [17].

To perform material nonlinearity analyses, plasticity behavior was based on the von-Mises yielding criteria and the associated flow rule. Isotropic hardening was assumed for the monotonic analysis, whereas kinematic hardening was assumed for the cyclic analysis as used by Mao et al. [27] and Ricles et al. [28]. For base metals, both bilinear and multi linear material responses were investigated based on the material properties given by SAC (2000) [17]. However, the analytical results showed that the use of multi linear response agree well with the experimental results. For weld metals a multi-linear material response based on the material property given by Mao et al. [27]and Ricles et al. [28] was used.

Nonlinear geometric analyses were performed through a small strain, large displacement formulation. The monotonic analyses were conducted by applying a monotonic vertical displacement load to the beam tip until more than 4 percent total rotation at column web center was achieved and the load history recommended by the AISC (2010a) [29] was utilized for cyclic analyses. When loads are applied only in the vertical direction, then the out of plane deformations (normal to the web) may not occur. Therefore, in order to ensure that buckling would occur due to instability of model, the imperfect model subjected to cyclic or monotonic loading was used. In this study, in order to determine the imperfect model, first the buckling mode shapes were computed in a separate buckling analysis and then were implemented to perturb the original perfect geometry of the model.

In order to verify the accuracy of the model, the experimental results of RC06 from SAC (2000) [17] were compared to the analytical results obtained from the finite element models in terms of applied load and rotation, plastic equivalent strain distribution and buckling modes. Figs 4 and 5 show these comparisons. As Fig. 4 shows the applied load-rotation curve obtained from the finite element analysis is in good agreement with the experimental one. Fig. 5 shows the plastic equivalent strain distribution at 5.5 percent rotation. In this figure high concentration of the plastic equivalent strain at the beam at the end of the flange plates is quite evident and is similar to what was achieved during the experimental test. Furthermore, at the same location the beam flange experienced a wide local buckling which is completely clear in the experimental test (Fig. 5).

It should be noted that the fracture prediction is the most questionable part of a finite element study. Because it is inherently a complicated phenomenon and is dependent on many parameters such as weld and base metal properties, weld defects, notch effects, weld quality and weld toughness. In this study it was assumed that the qualified welders and fabricators are employed and high fracture toughness weld metals are used (as these should be, based on the AISC [30], Specification for Structural Steel Buildings).Considering the fact that the locations of high level of strains have significant probability of premature fracture and by comparing the

finite element results obtained from the specimen RC06 with the experimental results presented by SAC (2000) [17] a failure criterion was assumed as follows:

The connection fracture occurs when the Von-Mises strains at the whole width of the beam flange (at the end of flange plate length) or at the entire width of the flange plates (at the column face level) exceed the strain associated with the ultimate strength of the materials, based on the material properties reported by SAC (2000) [17].A similar failure criterion also was used by other researchers (e.g. Saffari, et al. [31];Berman, et al. [32]). Note that the connection failure can also be predicted using rupture index, RI (e.g. Chao et al. [33]; Prinzet al. [34]). This index is defined as ratio between the plastic equivalent strain index and the ductile fracture strain. However, this method may be better when the fracture initiates from the beam web rather than the beam flange. Note that none of the mentioned methods are intended to predict exact rotation capacities for connections; rather, they provide a tool for comparing various models.

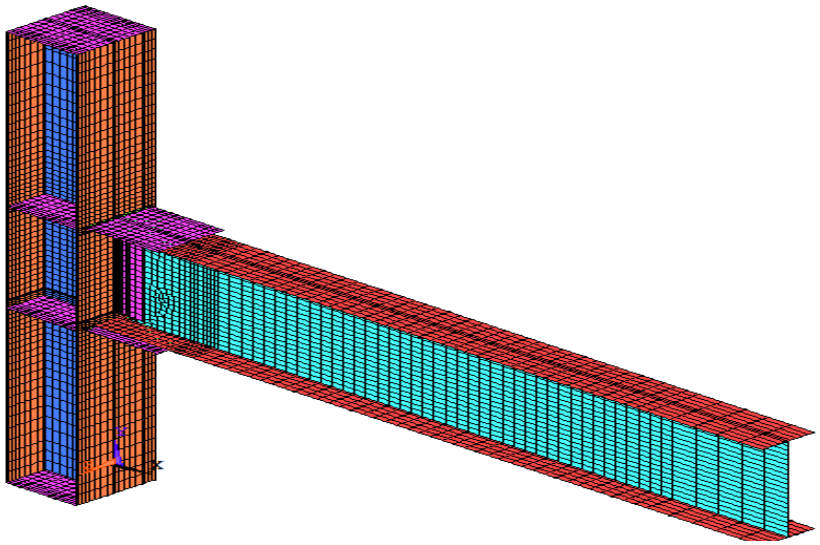

Figure 3. Finite element mesh of specimen RC06

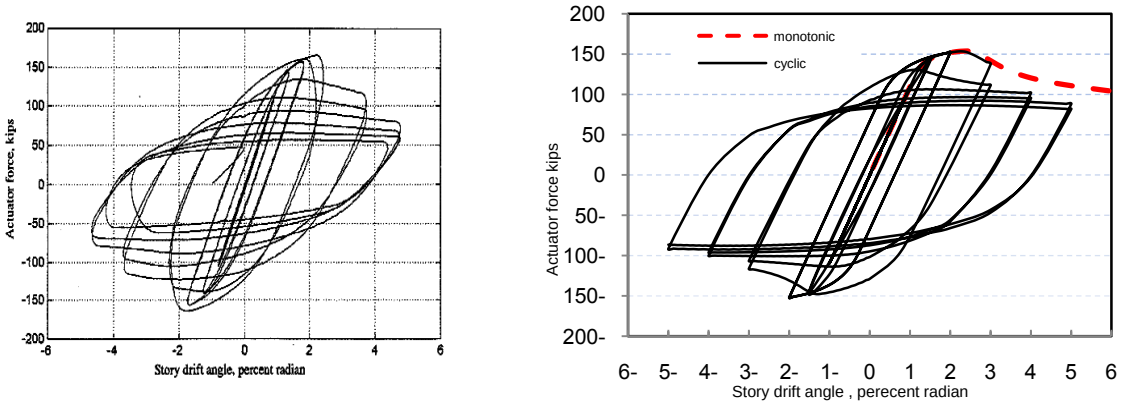

(a) Experimental test conducted by SAC (2000) (b) Finite element model

Figure 4. Applied force-rotation curve of specimen RC06 obtained from

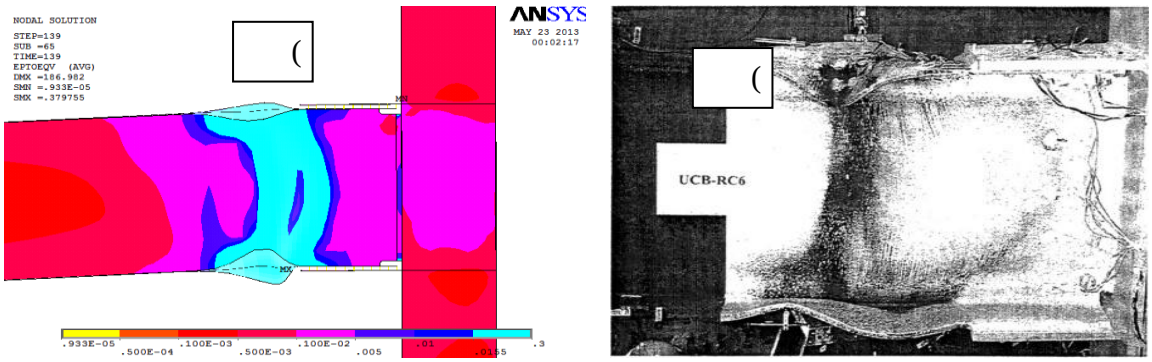

(a) Finite element model (b) Experimental test done by SAC (2000)

Figure 5. Plastic equivalent strain distribution of specimen RC06 obtained from

3. PARAMETRIC STUDY AND ANALYTICAL RESULTS

Proposed design procedures to modify pre and post Northridge connections are usually based on three beam sections: W36x150, W30x99 and W24x68. Therefore, all parametric studies were done on specimens SPE07 (beam: W36x150; column: W14x257), SPE05 (beam: W30x99; column: W14x176) and SPE03 (beam: W24x68; column: W14x120). These specimen sizes were chosen since they may be good representatives of the conventional pre/post Northridge specimen sizes, large, medium and small (Lee et al.) [35]and were also tested in phase 1 of SAC Steel Projects (SAC 1996) [36].The beam and column lengths of these specimens were similar to those that were used for specimen RC06. However, the configuration of these specimens was similar to the one that is shown in Fig. 2.

All specimen were designed based on the Iranian National Building code[37]and AISC[29,30]. To design the flange plates, the maximum applied moment at the column face (M_{cf}) was determined using equation 1. In this equation Z_b and f_{ye} are the beam plastic section modulus and the expected yield stress of the material respectively. S_c is equal to the length of the flange plate plus ¼ of the beam overall depth and V_{exp} is the expected shear force at the plastic hinge location. C_{pr} is a factor to account for the peak connection strength, including strain hardening, local restraint and additional reinforcement. In FEMA350 [12], the C_{pr} factor is given by equation $(f_y+f_u)/2f_y$, where $f_u$is the specified minimum tensile stress of the material. FEMA350 [12] proposes the use of value 1.2 for any case of modified connections except where otherwise noted in the individual connection design procedures. Similar to SAC [17], in the present study the value used for parameter C_{pr} was 1.1.

$$M_{cf} = C_{pr}.Z_b.f_{ye} + V_{\exp}.S_c \quad (1)$$

3.1 Effect of beam's material property on the connection behavior

Specimen RC06 of SAC (2000) [17] was constructed using high grade steel (i.e. A572 Grade 50 steel, yield stress =345 MPa). While the most common steel grade used in Iran, especially for beams, is A36 (yield stress=250 MPa). Hence the WFP connection SPE05was designed for both steel grades. Table 1 summarizes the details of these two specimens. For the top flange plate the width of the plate at the column face level is larger than the one at

the noise of the flange plate (width at the column face: 337 mm; width at the noise of the flange plate: 245 mm).

Fig. 6 compares the moment-rotation curves of the two specimens. As this figure shows by reducing the steel grade, initial rotational stiffness, strength and ductility of the connection increased. Both specimens could achieve the minimum required ductility. At four percent radian total rotation, the connection strength of both specimens was greater than the minimum required strength (i.e. M/M_P was greater than 0.8). However, the specimen of the higher steel grade showed lower strength and experienced faster strength degradation than the one of the lower steel grade. Therefore, investigation of the behavior of specimens of the higher steel grade (i.e. A572-Gr50) has been regarded more critical. Furthermore, using high grade steel is more desirable for designers. Sine it is the most economical way to increase the flexural capacity of beams without change in the beam section. Also in the case of having deep beams, using of high steel grade helps to reduce the beam overall depth. It finally leads to increase in the connection ductility and to reduce in the total height of the building. Hence, hereafter all parametric studies have been done using the high grade steel (A572-Gr50).

Table 1: Details of WFP specimens SPE05 with different beam material properties

Specimen SPE05	Material property			Flange plate dimension (mm)		Shear tab (mm)	Continuity plate (mm)
	Beam	column	Flange plate	top	bottom		
NO.1	A36	A572.Gr.50	A36	(337&245)x380x25	337x380x25	660x147x13	2x353x188x25
NO.2	A572.Gr.50	A572.Gr.50	A572.Gr.50	(337&245)x380x25	337x380x25	660x147x13	2x353x188x25

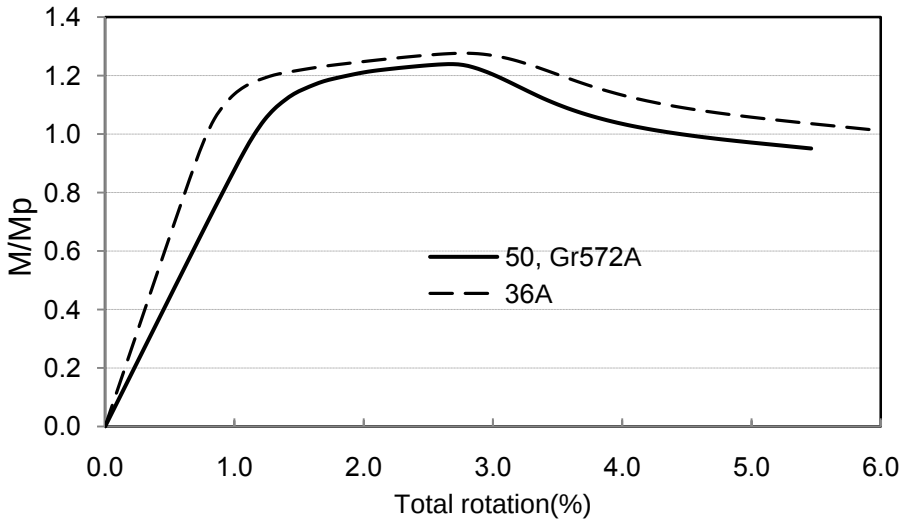

Figure 6. Moment-rotation curves of WFP specimen SPE05 for different beam material properties

3.2 Effect of the common methods to transfer the beam-column shear on the connection behavior

In this section the effects of the common methods to transfer the shear forces form the beam to the column flange on the connection behavior were investigated. The shear forces can be

transferred through: (1) Shear tab; (2) The top and the bottom rib plates; (3) The beam web which is directly welded to the column flange and (4) The top and the bottom flange plates. For initial investigation, specimen RC06 (with rectangular flange plates) was re-designed by considering the four methods mentioned above. In the first case the length, the width and the thickness of the shear tab plate were660 mm, 145 mm and 13 mm respectively. Fig. 7 shows the moment-rotation curve of this specimen. As this figure shows this specimen could achieve 5.5 percent total rotation while its strength at four percent total rotation was greater than one. It indicates the acceptable performance level of this specimen. In the second case, the shear force was transferred by totally four rib plates (two rib plates at the top and two of them at the bottom) with the dimensions of 15x100x200 mm which were connected to the beam flange and the column flange through the fillet welds. In this case, the connection only achieved 2 percent radian total rotation which is less than the minimum required total rotation (see Fig. 7). In the third case (i.e. direct welding of the beam web to the column flange), the connection achieved same strength and rotational capacity as those that were obtained for specimen RC06 in the first case. The worst behavior was achieved when shear force was transferred through the flange plates (forth case). In this case, the maximum total rotation was around 1.5 percent radian and the connection fracture occurred when it was in the elastic region (Fig. 7).

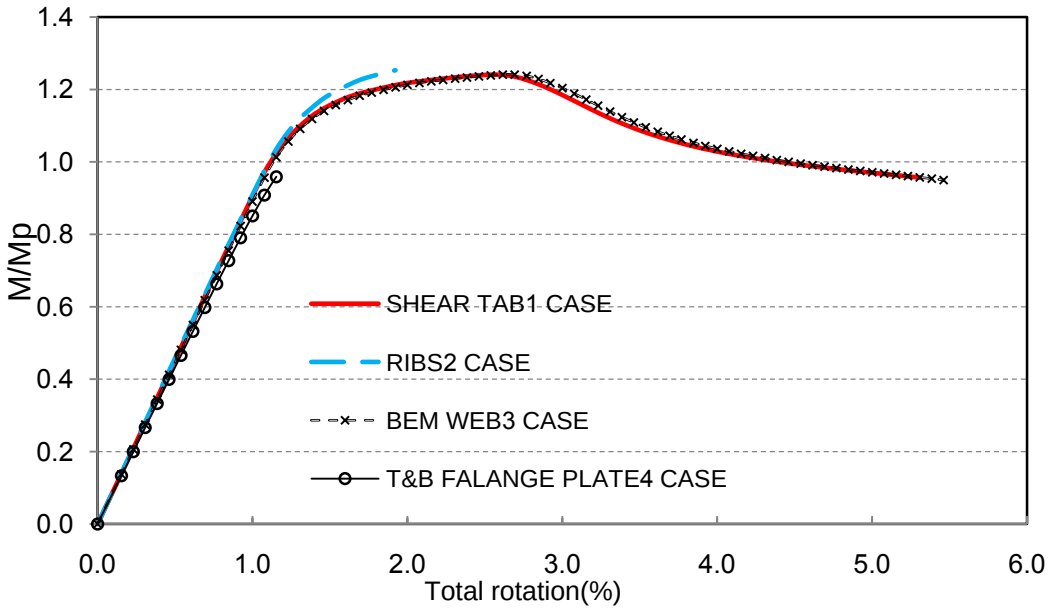

Figure 7. The moment-rotation curves in effect of common methods for beam- column shear transfer in specimen RC06

Direct welding of the beam web to the column flange (case 3) is an acceptable method to increase the connection ductility (FEMA355D) [24]. In this method shear force is properly transferred to the column flange through the beam web (not through the flange plates) and the beam web participates in the moment transferring. Hence, in this case the proper behavior of the connection is completely expected. In the fourth case all shear forces are transferred to the column flange through the flange plates. In this case the flange plates are

overstressed (due to the combination of the normal and the shear stresses) and consequently the early fracture of the flange plates happens. When case 1 and 2 are compared, it might be concluded that the use of the shear tab is a better method to transfer the shear forces. The question is if this is the case for any connection configuration.

Initial investigations showed that the connection ductility can also be a function of the connection length (the length of the flange plates, L_p) and the beam overall depth (d_b). Hence, by defining a non-dimensional parameter, L_P/d_b, the behavior of WFP connections was investigated. Tables 2 and 3 summarize the results of these specimens. In these tables θ_u and θ_d are the maximum total rotation achieved under upward loading and downward loading respectively and $\theta$is the lesser of the two values.

With reference to Tables 2 and 3, when L_P/d_b is greater than 0.6, generally using the rib plates was better than the use of the shear plate, whereas in L_P/d_b range which is less than 0.6, using the rib plates led to the brittle fracture at the face of the column in small rotation. The reason for this behavior might be explained as follows:

It is well known that in the welded connections at a region near the column face the classic beam theory is invalid (SAC 2000 [17]; Cheol [38]). In this region, shear stresses are at a maximum level near the column flanges, especially at the beam flange or at the flange plate area. Generally, the combination of the shear stresses and the normal stresses at the beam flanges near the column face causes high tri-axially stress at the face of the column and consequently it promotes the brittle fracture of the welded connections. Based on this discussion, the distribution of the Von-Mises strains (which is a combination of the normal and the shear strains) for WFP connections were compared in two main cases, L_P/d_b less than 0.6 and greater than 0.6.

For instance, Figs. 8.a and 8.b compare the normalized von-Mises strain (von-Mises strain divided by the yield strain) distributions at the center line of the top and the bottom flange plates along the beam length for specimens SPE05 and RC06 respectively. These curves are drawn for two different methods used to transfer the shear forces (i.e. using shear tab and rib plates) when the ratio of the L_P/d_b is 0.5 (L_P=380mm, d_b =750 mm). As these figures show, for the top flange plates, there is no significant difference between the von-Mises strain distribution curves when the shear forces are transferred either through the shear tab or the rib plates. However, it was not the case for the bottom flange plates. There can be seen a common behavior for both bottom flange plates regardless of the method used to transfer the shear forces. For both methods:

- By moving from the end of the flange plate towards the column face the von-Mises strains gradually increased which is due to the increase in the applied moments.
- There was a sudden increase in the von-Mises strains at the vicinity of the column face which was due to the presence of the shear strains and the associated secondary normal strains at the flange plates due to the improper transformation of the shear forces through the beam web. However, for both SPE05 and RC06 specimens, this increase was much more when the rib plates were used to transfer the shear forces.

Figs 9.a and 9.b compare the normalized von-Mises strain distributions at the center line of the top and the bottom flange plates along the beam length for specimens RC06 and SPE05 respectively when the L_P/d_b ratio is 1.0 (L_P=750 mm, d_b =750 mm). Similar to the previous case, for the top flange plates, there is no significant difference between their von-Mises strain distribution curves when the shear forces are transferred either through the

shear tab or the rib plates. As Figs. 9.a and 9.b show, for the bottom flange plates, by moving from the end of the flange plate towards the column face, the Von-Mises strains gradually increased. Again a sudden increase can be seen in the von-Mises strains at the vicinity of the column face which are due to the presence of the shear strains and the associated secondary normal strains at the flange plates. However, in contrast to the previous case, for both SPE05 and RC06 specimens, this increase was much less when the rib plates were used to transfer the shear forces.

These might be the reasons of facing of different connection behaviors when L_P/d_b is more or less than 0.6. Similar behaviors were also observed for WFP connections SPE07.

Table 2: Effect of L_P/d_b ratio on the connection's strength and ductility when the shear tab is used

Specimen	L_P (cm)	L_P/d_b	θ_u (%)	θ_d (%)	θ (%)	M/MP at 4% total rotation	M/MP at failure time
RC06	38	0.51	5.5	5.5	5.5	1.01	0.93
	48	0.64	5.3	5.3	5.3	1.05	0.97
	60	0.8	5.2	5.2	5.2	1.12	1.04
	75	1	2.7	2.7	2.7	1.19	1.04
SPE05	32	0.43	5.5	5.5	5.5	1.02	0.92
	38	0.51	5.5	5.5	5.5	1.04	0.95
	48	0.64	6	6	6	1.09	0.97
	60	0.8	6	3.8	3.8	-	1.16
	70	0.93	6	3.7	3.7	-	1.41
	75	1	3.5	3.7	3.5	-	1.41
SPE07	40	0.44	4.7	4.7	4.7	1.11	0.91
	50	0.55	5.2	5.1	5.1	1.27	1.1
	70	0.76	4.7	5.7	4.7	1.29	1.16
	80	0.87	2.9	1.9	1.9	-	1.37
	90	1	2.7	2.7	2.7	-	1.34

Table 3: Effect of L_P/d_b ratio on the connection's strength and ductility when the rib plates are used

Specimen	L_P (cm)	L_P/d_b	θ_u (%)	θ_d (%)	θ (%)	M/MP at 4% total rotation	M/MP at failure time
RC06	38	0.51	1.9	1.9	1.9	-	1.17
	48	0.64	5.2	5.2	5.2	1.03	0.96
	60	0.8	4.6	4.6	4.6	1.08	1.03
	75	1	4.9	4.9	4.9	1.1	1.38
SPE05	38	0.51	1.9	1.9	1.9	-	-
	48	0.64	5.8	5.8	5.8	1.07	0.95
	60	0.8	6	6	6	1.14	1.04

	70	0.93	6	6	6	1.33	1.15
	40	0.44	1.69	1.69	1.69	-	1.12
	50	0.55	5.5	5.6	5.5	1.14	0.97
SPE07	70	0.76	4.9	5.2	4.9	1.16	1.07
	80	0.87	5.2	5.4	5.2	1.19	1.09
	90	1	5.4	6	5.4	1.21	1.1

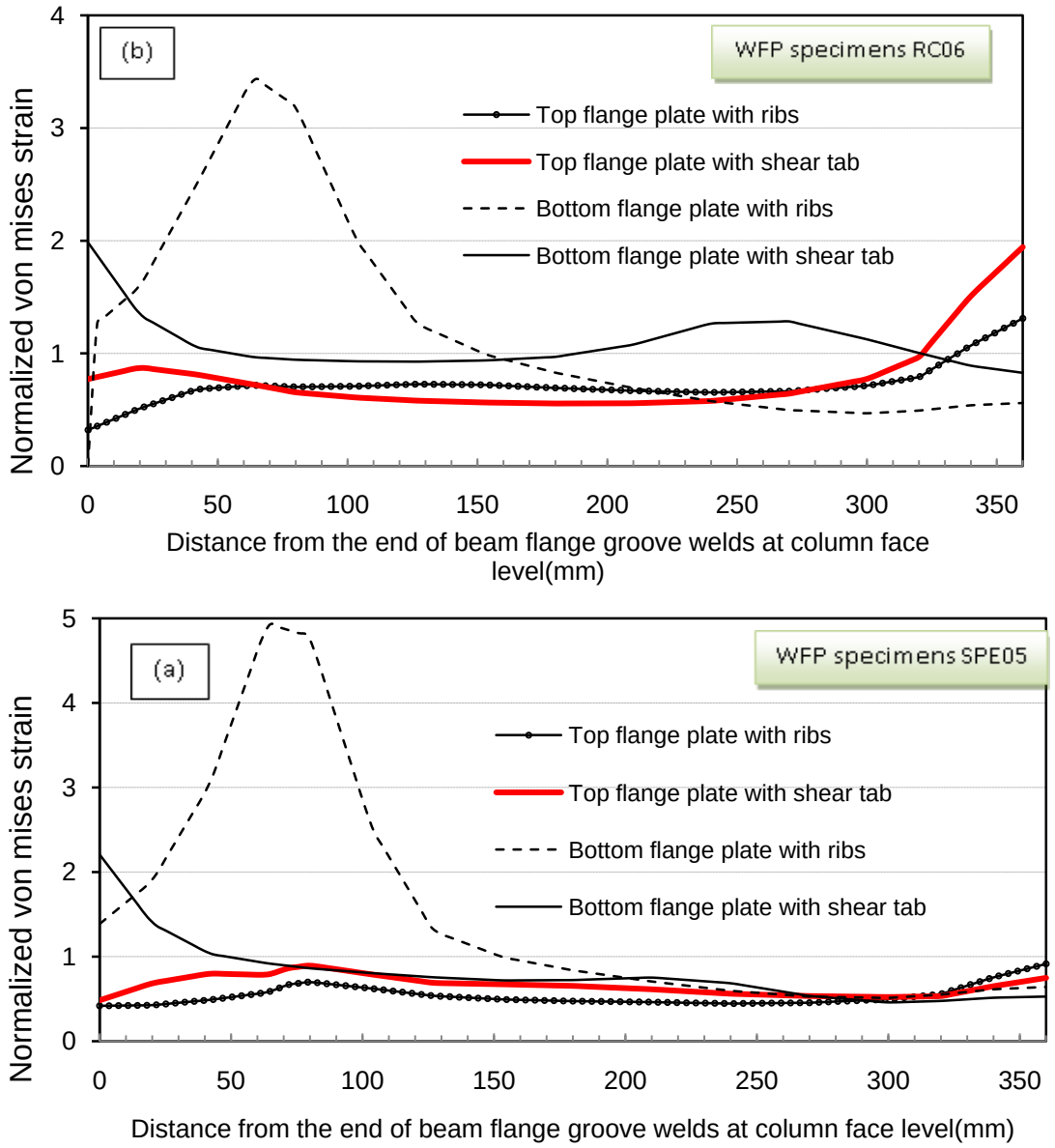

Figure 8. Normalized von-Mises strain distribution along the center line of the top and bottom flange plates when L_p/d_b=0.5 for the WFP specimens: (a) SPE05; (b) RC06

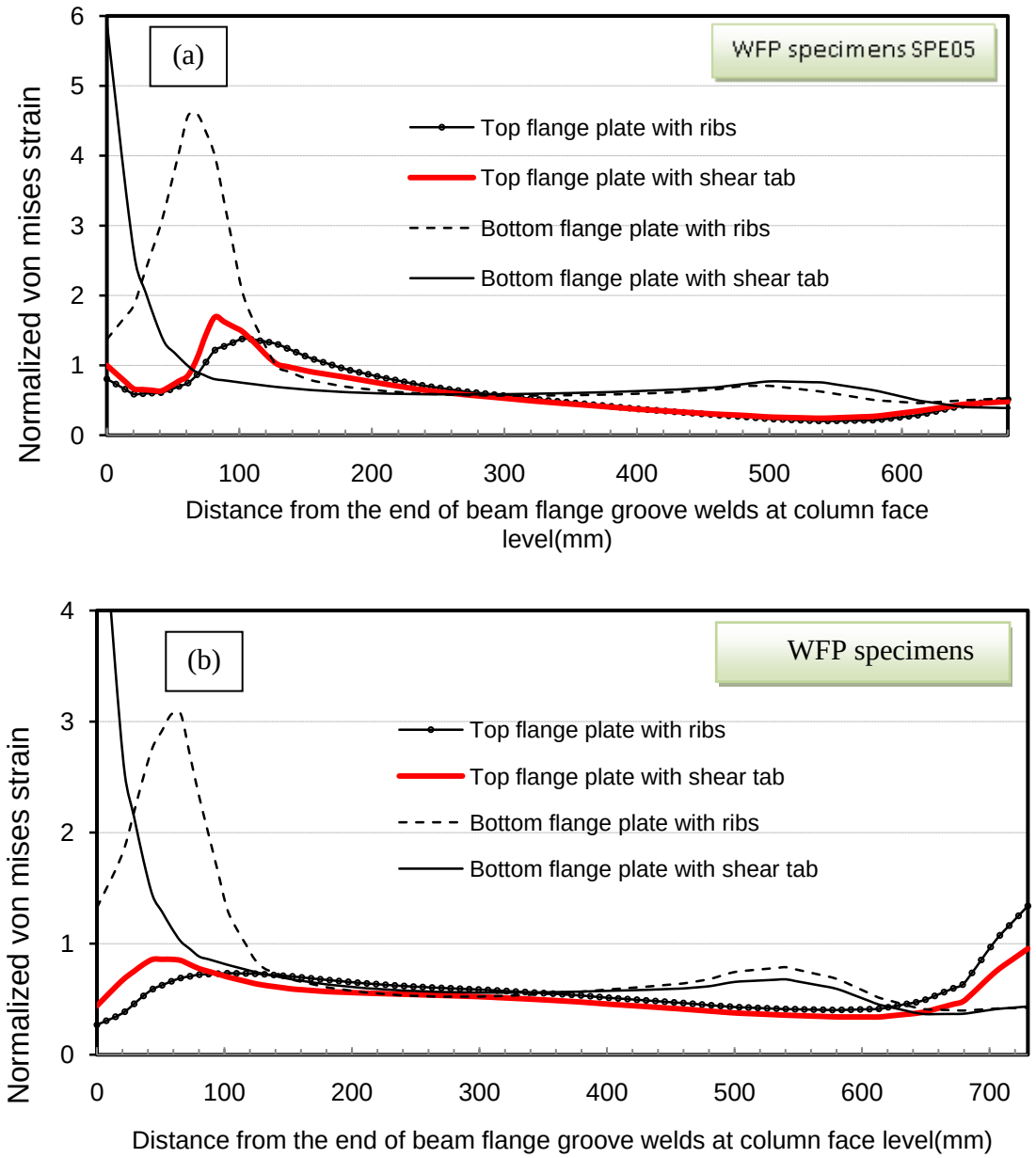

Figure 9. Normalized von-Mises strain distribution along the center line of the top and bottom flange plates when $L_P/d_b=1$ for the WFP specimens: (a) SPE05; (b) RC06

3.3 Effect of the transverse welding at the noise of the flange plates on the connection behavior

In order to evaluate the effect of the transverse welding on the connection behavior, specimen RC06 was designed and modeled with and without transverse welds. Note that in this study fillet welds were not explicitly modeled but their effects were considered using couple command in the ANSYS program. In this case the degree of freedom of the nodes at

the intersection of the noise of the flange plates and the beam flange plate were coupled together.

Fig. 10 compares the normalized Von-Mises strain distribution across the beam flange and the flange plate at the various levels in the presence and the absence of the transverse welds for the WFP specimen RC06 at 6% total rotation. As Fig. 10.a shows the presence of the transverse welds was ineffective to reduce the normalized strains across the flange plate at the column face level. At this location the maximum von-Mises strain was very low and was around 1.1 times of the yield strain of the flange plate material. However, as Fig. 10.b shows the presence of the transverse weld caused a significant reduction in the normalized strains across the beam flange width at the noise of the flange plate. It was due to the composite function of the beam flange and the flange plate to resist the von-Misesstrains.By moving from the noise of the flange plate towards the plastic hinge length, this positive effective reduced such that at 40 mm away from the noise of the flange plate the presence of the transverse welds were somehow ineffective (Fig. 10.c). By moving more inside the plastic hinge length, the presence of the transverse welds became detrimental (Figs. 10.d and 10.e) such that at a distance equal to 100 mm away from the noise of the flange plate the presence of the transverse welds causes10 percent increase in the beam flange strains in compare to the specimen without beam transverse welds. It finally caused that the specimen with the transverse welds to show a lower ductility than the one without the transverse welds (Fig. 11).However, their strengths are approximately the same. Based on these results it canbe concluded that to avoid the strain concentration at the plastic hinge area and to increase the connection ductility, only longitudinal welds to be used to connect the top flange plates to the beam flange. However, using the transverse welds can be effective in reducing the size of the fillet welds and consequently in reducing the thermal stresses at this location.

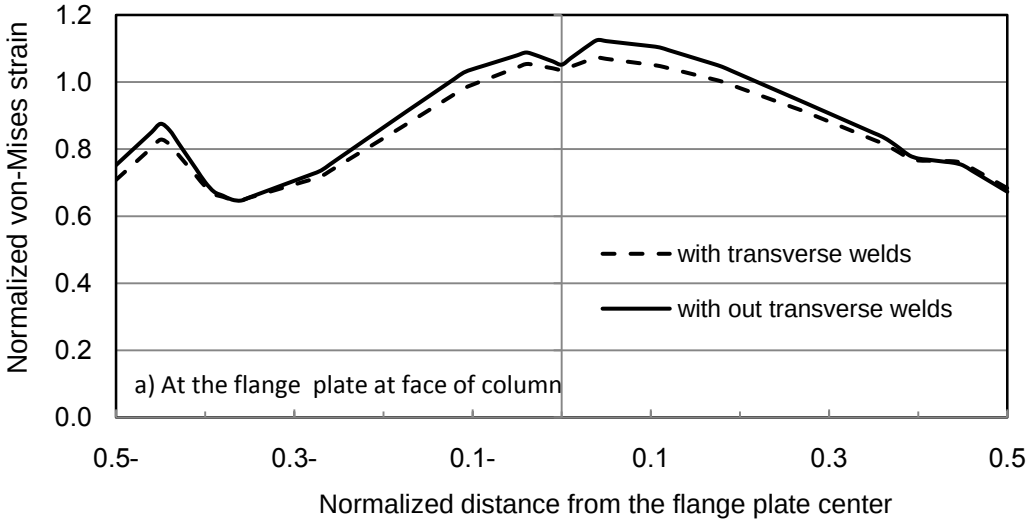

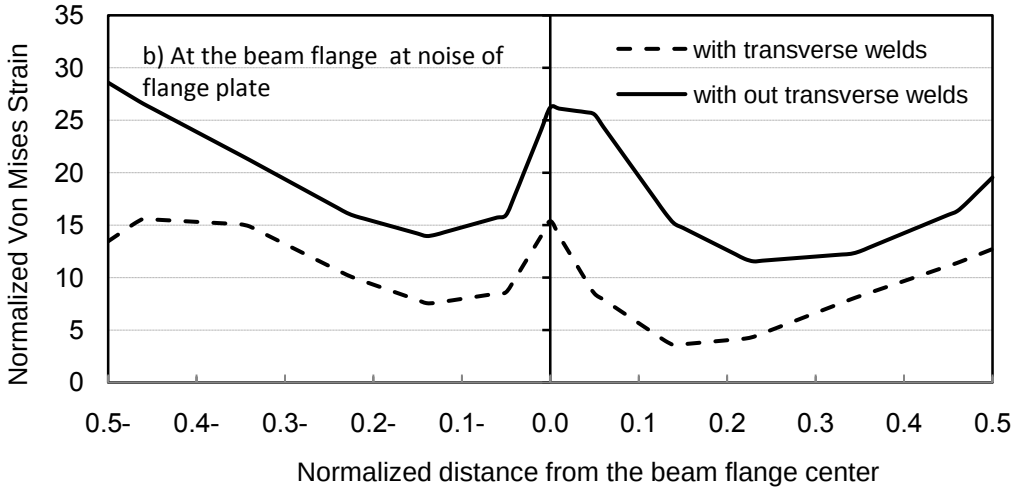
b) At the beam flange at noise of flange plate
with transverse welds
with out transverse welds
Normalized Von Mises Strain
35
30
25
20
15
10
5
0
0.5- 0.4- 0.3- 0.2- 0.1- 0.0 0.1 0.2 0.3 0.4 0.5
Normalized distance from the beam flange center

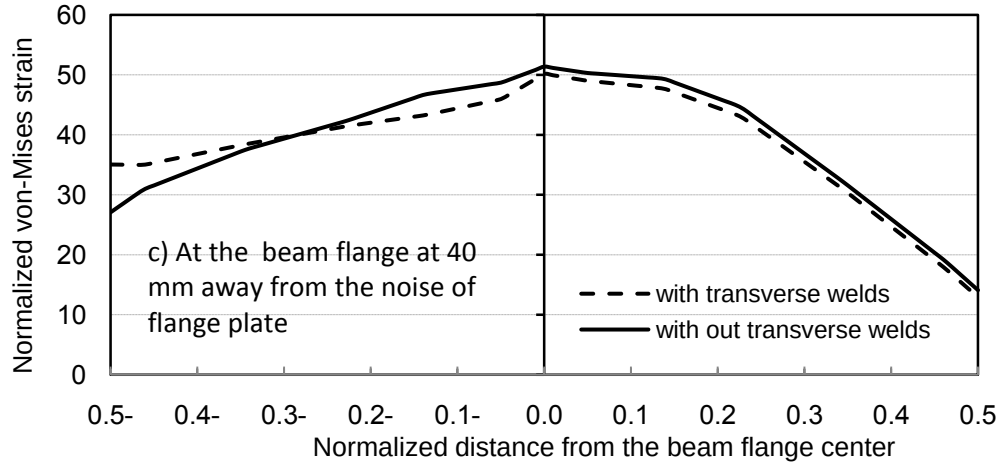
c) At the beam flange at 40 mm away from the noise of flange plate
with transverse welds
with out transverse welds
Normalized von-Mises strain
60
50
40
30
20
10
0
0.5- 0.4- 0.3- 0.2- 0.1- 0.0 0.1 0.2 0.3 0.4 0.5
Normalized distance from the beam flange center

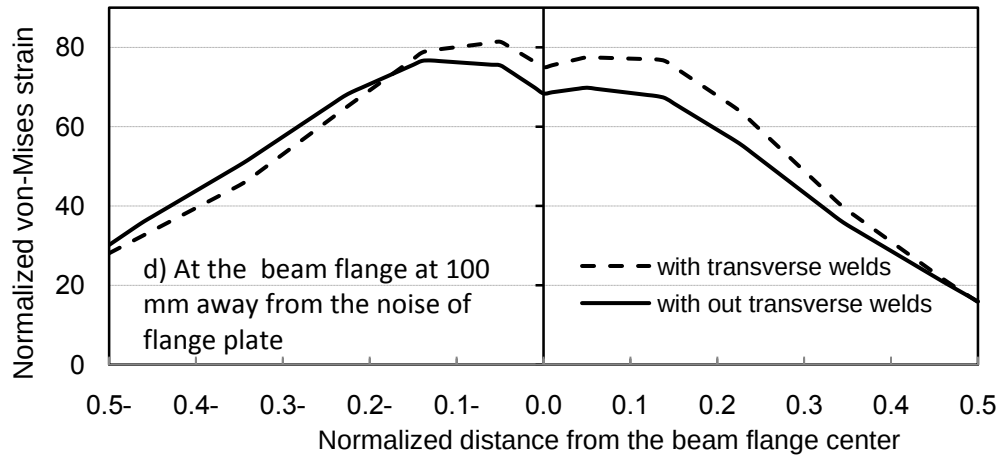
d) At the beam flange at 100 mm away from the noise of flange plate
with transverse welds
with out transverse welds
Normalized von-Mises strain
80
60
40
20
0
0.5- 0.4- 0.3- 0.2- 0.1- 0.0 0.1 0.2 0.3 0.4 0.5
Normalized distance from the beam flange center

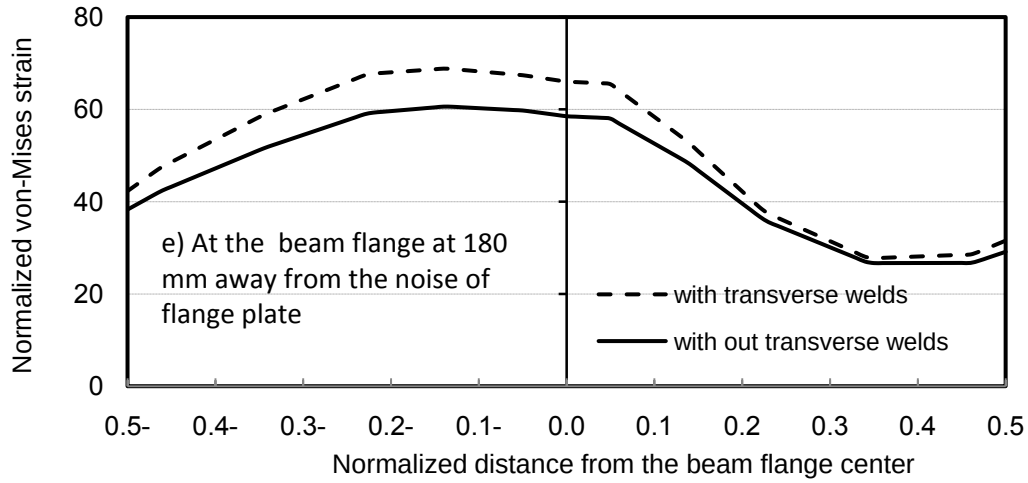

Figure 10. Normalized von-Mises strain distribution across the beam flange and the flange plate at various distances away from the column face

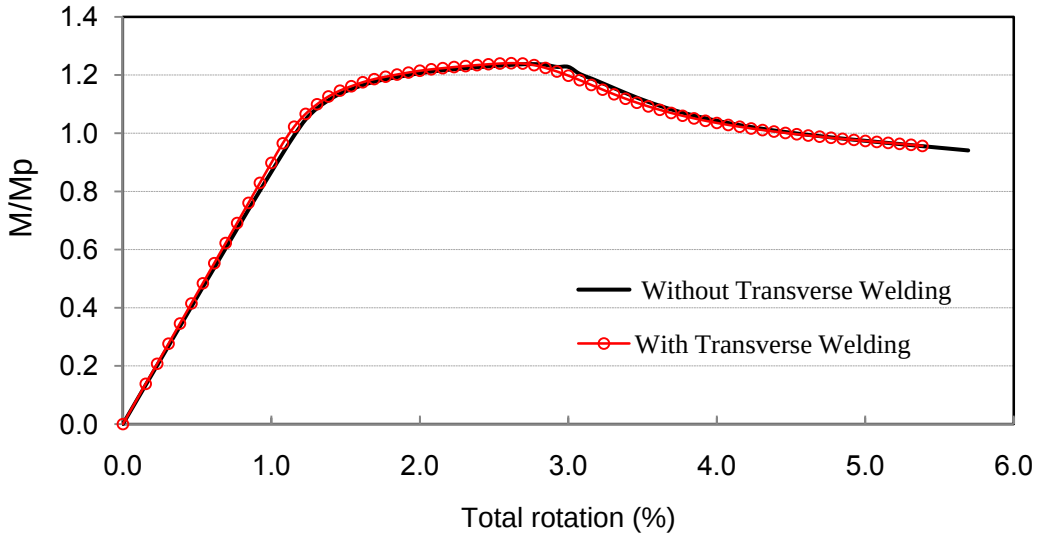

Figure 11. Moment-rotation curves of WFP specimens RC06 with and without transverse welds

3.4 Effect of the end form of the top reinforcing plate on the connection ductility

As mentioned before, in Iran, in order to avoid overhead welding, the common used form of the top flangeplate is a combination of the trapezoidal and the rectangular form (Fig. 2). Hereafter for simplicity, this form of the top flange plate is named as TR form. In FEMA350 (2000) [12], the top flange plate has a rectangular form and its width is larger than the beam flange width. In this section the effect of the different forms of the top flange plate on the ductility of specimen SPE05 was assessed. Fig. 12 compares the Von-Mises strain distribution for these flange plates and their details are summarized in Table 4.

Table 4: Details of different forms of the top flange plate

Form	L_P (mm)	$t_{top\ plate}$ (mm)	$t_{bottom\ plate}$ (mm)	$b_{top\ plate}$ (mm)		$b_{bottom\ plate}$ (mm)	θ (%)	M/Mp at 4% total rotation
				at Start	at End			
1	380	25	25	337	337	337	5.31	0.96
2	380	36	25	337	245	337	5.39	0.95
3	380	36	25	337	245	337	5.25	0.99
4	380	36	25	337	245	337	5.15	0.99
5	380	36	25	337	130	337	4.7	0.95
6	380	36	25	245	245	337	5.31	0.96

Forms 1 and 2 are the same as those are presented in the FEMA350(2000) [12] and the Iranian steel code respectively. Comparing the von-Mises strain distributions of these two forms shows that the maximum strain developed for the FEMA350 (2000) [12] form is at the beginning of the flange plate (i.e. at column face level) and is $11.3\varepsilon_y$ where ε_y is the yield strain of the flange plate material. By using the TR form, the maximum Von-Mises strain decreased which is due to its higher thickness in compare to the one of the FEMA350 form. In this case, the maximum strain concentration occurred at the intersection of the rectangular and the trapezoidal parts (named as SC point).However, these differences between the first and the second forms did not affect the connection ductility (see Table 4) since in these connections the failure was due to the beam flange fracture at the plastic hinge area (beyond the noise of the flange plates) rather than at the flange plates. Fig. 13 compares the normalized Von-Mises strains across the beam flange width at the plastic hinge area at 6% total rotation. This figure clearly shows the high level of strains at this area in compare to the column face level. Also this figure indicates that the change of the top flange plate form did not have any effect on the strain distribution across the beam flange at the plastic hinge area.

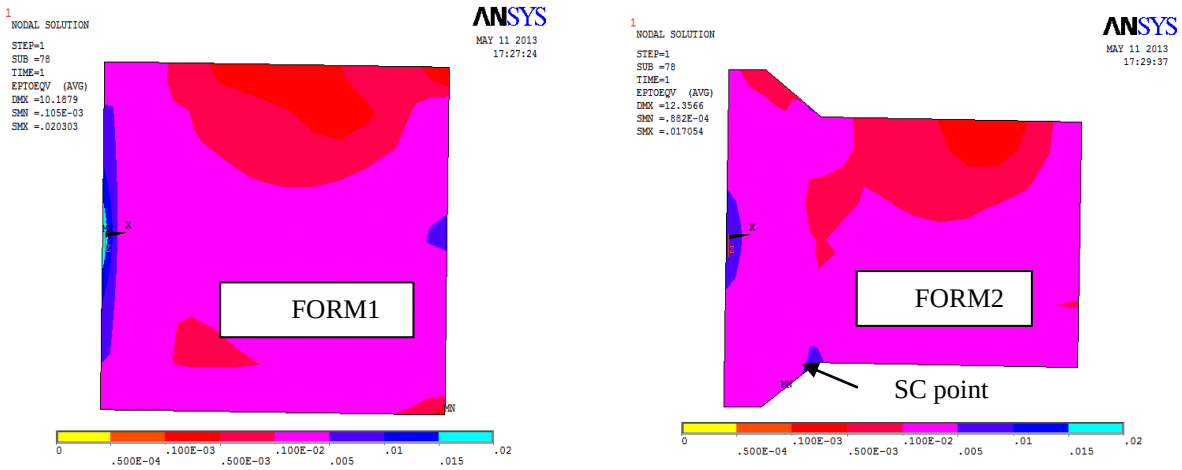

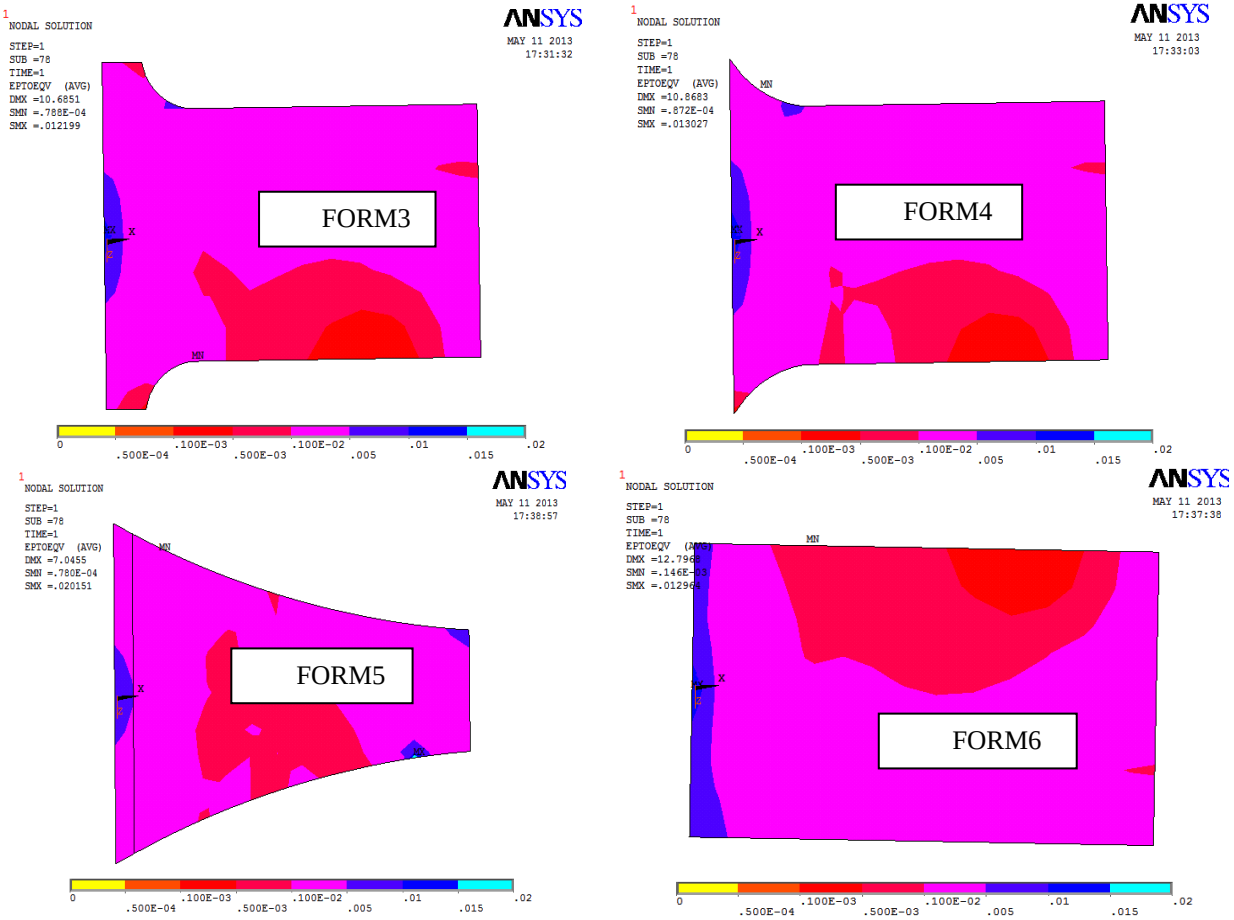

Figure 12. Von-Mises strain distribution for different forms of the top flange plate

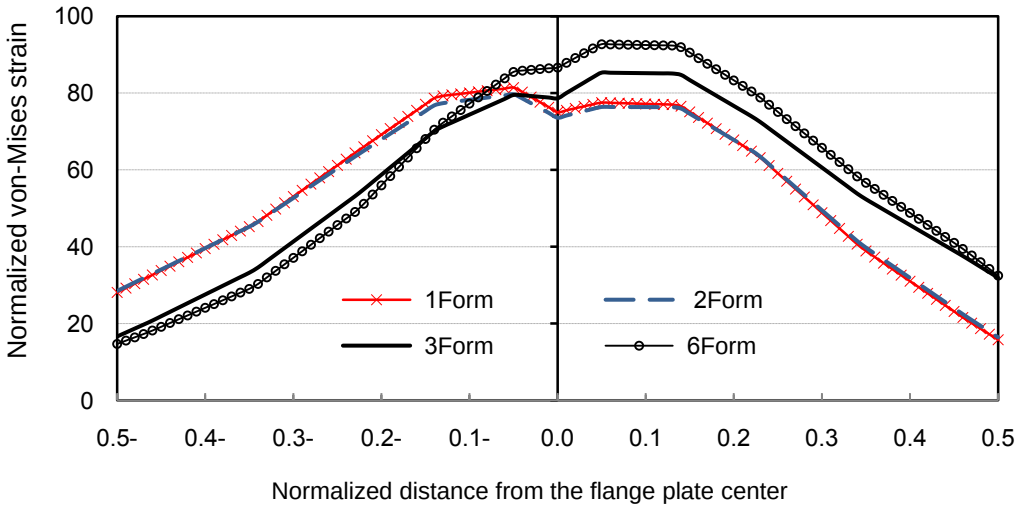

Figure13. Normalized von-Mises strain distribution across the beam flange at 100 mm away from the noise of the top flange plate for WFP specimens SPE05

It should be noted that the strain concentration at the SC point can be detrimental if a crack exist at this point which can easily be created during the fabrication of the top flange plates of the TR form. In this case the stress intensity factor (SIF) may easily exceed the fracture toughness of the flange plate metal and finally leads to a brittle fracture at this point. Note that in the finite element modeling the cracks were not considered and the SIFs were not calculated.

To avoid such brittle failure, in the forms 3 through 5, it was tried to remove the SC point. As Fig. 12 shows by rounding the sharp corner at the SC point, the maximum strainof forms 3 and 4 reduced to $6.7\varepsilon_y$ and $7.2\varepsilon_y$ respectively. While the fifth form was ineffective to reduce the maximum Von-Mises strains and also achieved the lowest ductility among the other forms (see Table 4). Note that the width of this flange plate at its tip was approximately half of the beam flange width and it caused a higher strain concentration at the plastic hinge areawhich promoted the beam flange fracture at this region. The sixth form of the top flange plate is the same as the first form except that its width is less than the beam flange width and consequently its thickness is larger than the one of the first form. This form of the flange plate also avoidsthe overhead welding of the rectangular flange plate to the beam flange. For this form, the connection ductility was 5.3 percent total rotation. This form caused highest von-Mises strain concentration across the beam flange at the plastic hinge area in compare to the other forms (Fig. 13).

As the results presented in this sectionshowed, generally there is no remarkable difference between the connection's ductility and strength of the WFP connections of different form of the top flange plate. However, when the connection fabrication follows the common practice in Iran, among the investigated forms, the third one might be the best form. Since it reduced the strain concentration at SC point and avoids the overhead welding. But when the connection fabrication is similar to the American code of practice, still the first form is the most desirable one since the flange plate thickness is in a minimum level which results in lower cost and thermal stresses at the column face level.

3.5 Effect of equality and inequality of the top and the bottom plate length on the connection ductility

The lengths of the top and the bottom flange plates are a function of the required weld length to connect these plates to the beam flange plates. Generally, in the case of using a flange plate of the TR form, the initial part (the trapezoidal part) is not welded to the beam flange and it causes the weld length of the top flange plate to be less than the bottom one. In this case, in order to avoid increasing the fillet weld sizes, in many designs the top plate length is considered longer than the bottom one while for the WFP connections presented in FEMA350 [12], these plates have same length. In this section the effect of the inequality of the top and the bottom flange plate lengths on the connection ductility was investigated. Note that in this section due to the asymmetry shape of the connection; all specimens were analyzed under both upward and downward loading. Fig. 14 shows the moment-rotation curves of specimen SPE05 for three different cases where the length of the top or the bottom flange plates are either 48 cm or 38 cm. Note that in all cases the shear force was transferred to the column flange through the shear tab.

As this figure shows, under upward loading, when the top flange plate is longer, the connection achieved a higher rotational capacity and experienced lower strength degradation

when it is compared with the one with the top and bottom flange plates of the same length. However, under downward loading, when the top flange plate is longer, the relevant moment-rotation curve doesn't show a better rotation and mostly indicates much more strength reduction when it is compared to the one of the top and bottom flange plates of the same length.

When the top flange plate is shorter than the bottom flange plate, under downward loading, this specimen experienced same rotational capacity and strengthas that was obtained for specimen of the equal flange plate lengths. However, under upward loading, when the top flange plate is shorter, the relevant moment-rotation curve doesn't show a better rotation and mostly indicates much more strength reduction when it is compared to the one of the top and bottom flange plates of the same length.The same results have been observed in assessing the specimen SPE07. Therefore, it might be concluded that for the both upward and downward loading, the best connection performance may happen when the length of the both top and bottom flange plates are equal.

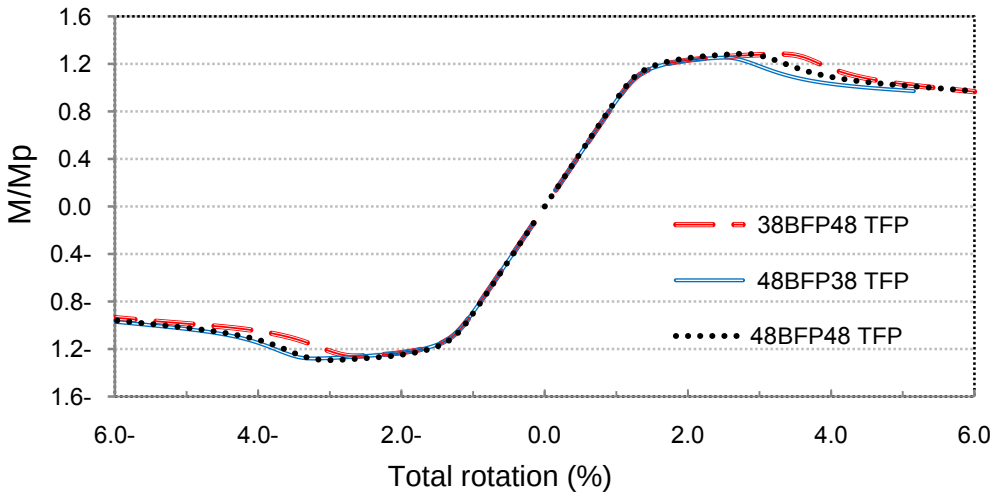

Figure 14. Moment-rotation curves of WFP specimens SPE05 in case of using different length for the top and the bottom flange plates

3.6 Effect of the rib plate form on the connection ductility

In this section the effects of rib plate dimension on the strength and ductility of specimens RC06, SPE05 and SPE07 were investigated. Fig. 15 shows the details of the different types of used rib plates. For instance, Table 5 summarizes the results for WFP specimens RC06. In this table H_{rib}, V_{rib} and t_{rib} are the horizontal length, the vertical length and the thickness of the rib plates respectively. Rib plates of type 1 have the smallest horizontal length and were named as shear rib plates. While the rib plates of type 4 and 5 have the largest horizontal length and were named as flexural rib plates. As this table shows, for both values of the L_P/d_b ratio, by increasing the horizontal length of the rib plates (using flexural rib plates), both the connection's strength and ductility increased. Similar behavior was also observed for specimens SPE05 and SPE07. Based on these results it can be recommended that for the WFP connections where the L_P/d_b ratio is less than 0.6 (i.e. for short flange plates), the horizontal length of the rib plates must be equal to the flange plate length

(H_{rib}/L_P=1). While in the case of using long flange plates (L_P/d_b>0.6), the rib plates must have a minimum H_{rib}/L_P equal to 0.6. Fig. 16 compares the moment-rotation curves of the WFP specimens RC06 with the shear and the flexural rib plates. This figure clearly shows a delay in the onset of the beam flange and web local buckling (i.e. the onset of the strength degradation) when the horizontal length of the rib plates were increased. It finally led to an increase in both the connection's strength and ductility.

Table 5: Strength and ductility of WFP specimens RC06 with various rib plates

Specimen	Rib plate type	L_P (mm)	L_P/d_b	H_{rib}(mm)	v_{rib} (mm)	t_{rib}(mm)	H_{rib}/L_P	Number of ribs	θ(%)	M/Mp at failure time
RC06	1	380	0.51	100	200	15	0.26	4	1.92	1.17
	2	380	0.51	200	200	15	0.53	4	2.6	1.2
	3	380	0.51	300	200	15	0.79	4	2.8	1.25
	4	380	0.51	380	200	15	1	4	3.08	1.11
	5	380	0.51	380	200	15	1	4	3.08	1.11
	1	480	0.64	100	200	15	0.21	4	5.15	0.96
	2	480	0.64	200	200	15	0.42	4	5.38	0.97
	3	480	0.64	380	200	15	0.79	4	6	1.08

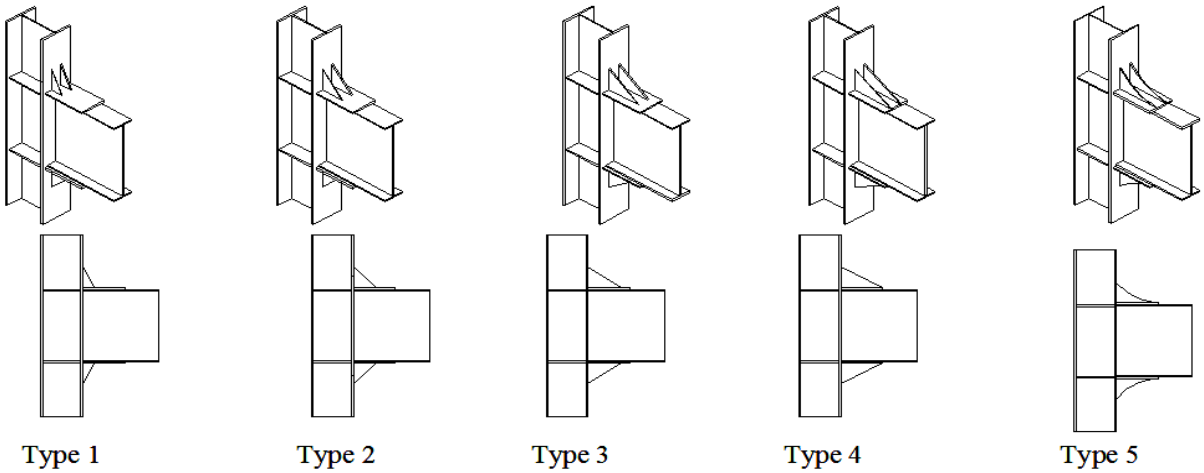

Figure 15. Details of the various types of the used rib plates

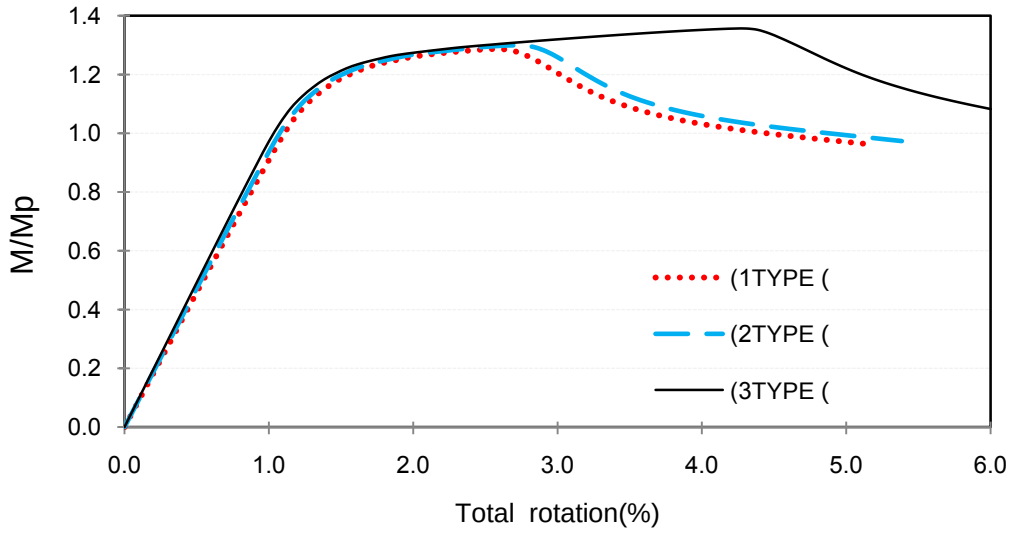

Figure 16. Moment-rotation curves of the WFP specimens RC06 (L_P=48 cm)with the shear and the flexural rib plates

4. SUMMARY OF RESULTS

Evaluation of the WFP connections presented in the previous section revealed that these connections generally can achieve adequate rotational capacity (i.e. total rotation greater than 0.04 rad) provided that:

1. The length of the top and the bottom flange plates is same.
2. Depends on the ratio of the L_p/d_b, the appropriate method is used to transfer the shear forces.
3. Depends on the fabrication method, the appropriate form of the top flange plate is used (i.e. forms 1 and 3).
4. Flexural rib plates are used when the shear forces are transferred through the rib plates.

As mentioned before, the connection strength can be evaluated using M/M_P ratio. Based on the seismic provision (AISC) [29], from the strength point of view, a connection is acceptable if the measured flexural resistance of the connection determined at the column face, is at least $0.80M_P$ of the connected beam at a story drift angle of 0.04 rad. Generally connections show higher strength degradation when they are subjected to the cyclic loading[9]. Examination of the RC06 cyclic and monotonic analyses (Fig. 4.a), it was found that the ratio of the connection strength under the cyclic loading to the one under the monotonic loading at 4 percent total rotation is equals to 0.71. Hence, it might be concluded that the connection strength obtained from the monotonic analysis can be turned to the cyclic one by multiplying to a reduction factor equal to 0.71. Note that in the previous section, all the presented results were obtained based on the monotonic loading. This indicates that all the connection strengths presented in the previous section must be modified by multiplying to a reduction factor of 0.71. With respect to this issue, the strength at four percent total

rotation of a WFP connection of the recommended configuration listed above is between 0.77 and 0.9 which is so close to the minimum required strength, 0.8.However, all WFP specimens tested by SAC 2000 [17] and Whittaker et al. [15] experienced even higher strength degradation. For instance the M/M_P ratios at four percent total rotation for specimens RC06 (beam section = W30x99) and FUSD1 (beam section =W21x50) 0f references SAC 2000 [17] and Whittaker et al. [15] were 0.71 and 0.7 respectively. These indicate that the proposed recommendations listed above were effective to enhance both of the connection strength and ductility simultaneously where relatively deep beams were used.

It should be noted that in the experimental tests done by Gholami et al. [23] and Ghobadi et al. [21], such significant strength degradation was not reported for WFP specimens LF30 (beam section=I380x200x12x8, beam depth =380 mm) and RC2 (beam section=IPE270, beam depth=270mm) respectively. The M/M_P ratios at four percent total rotation for specimens LF30 and RC2 were 1.1 and 1.25 respectively. The main differences between the sections used by these researchers were the beam overall depth and the slenderness ratios of the beam web and flange. In compare to the sections used by SAC 2000 [17], Gholami et al. [23] and Ghobadi et al. [21] used shallow beams of very compact flange and web.

Based on this discussion, it might be concluded that for a WFP connection of deep beam, which is designed based on the recommendations presented in the previous section, its strength is of concern rather than its ductility. Based on the experimental results of the specimens RC06, FUSD1 and LF30 and the finite element results of the specimens SPE03, SPE05 and SPE07, the main reason of the connection strength reduction is the local buckling of the beam flange and web at the plastic hinge area which finally leads to the beam flange fracture at this region. Therefore, in case of using a strategy to control the flange and web buckling at this region, higher connection strength can be expected. In the following section effects of using doubler plates at the beam web area to control the local buckling of the beam elements are investigated.

5. ADDING DOUBLER PLATES AT THE BEAM WEB AREA

For the WFP connections the beam web buckling is generally followed by the beam flange buckling and it finally leads to the beam flange fracture at the plastic hinge region. Hence, the beam flange fracture at the plastic hinge region might be controlled if the beam web is strengthened using a doubler plate. This strengthening method is shown in Fig. 17, where the thickness of the doubler plate is 5 mm.

The maximum height of the doubler plate (H_{dp}) was determined using $H_{db}=d_b-2k$ formula, where d_b and k are the beam overall depth and the distance from the outer face of the beam flange to the web toe of the fillet respectively. The length of the doubler plate (L_{dp}) was defined as a function of parameter b ($L_{dp}=100$ mm $+b$) and was located in such a way that 100mm of that, was located before the noise of the flange plate (Fig. 17).

Fig. 18 compares the moment-rotation curves of specimens RC06 (L_P=380mm) under monotonic loading for four cases: without doubler plate and with doubler plate when the parameter b is equal to 100 mm, 200 mm and 300 mm which are corresponded to the b/d_b ratio equal to 0.13, 0.27 and 0.4 respectively (d_b is the beam overall depth). As Fig. 18 shows the presence of the doubler plate was effective to increase the maximum connection

flexural capacity. It also caused a remarkable increase in the connection strength at four percent total rotation such that at this point the ratio of the M/M_P increased from 1.04 to 1.21when $b/d_b$was equal to 0.27.By increasing the doubler plate length (or b/d_b ratio) the connection strength increased. However, it caused a reduction in the connection ductility. This investigation was also carried out for specimens SPE03 and SPE07 where the beam overall depth of these specimens was 600 and 912 mm respectively. Table 6 summarizes the results of these specimens. In this table, M/M_P is the connection strength at four percent total rotation under cyclic loading and θ is the total rotation of connection at failure time. The results of this table clearly show the efficiency of the doubler plate to enhance the strength of all WFP specimens. However, as this table shows excessive increase in the horizontal length of the doubler plate was detrimental and caused a significant reduction in the connection ductility. Based on these limited results it might be concluded that the optimum value for b/d_b ratio to achieve both adequate connection strength and ductility is 0.13.

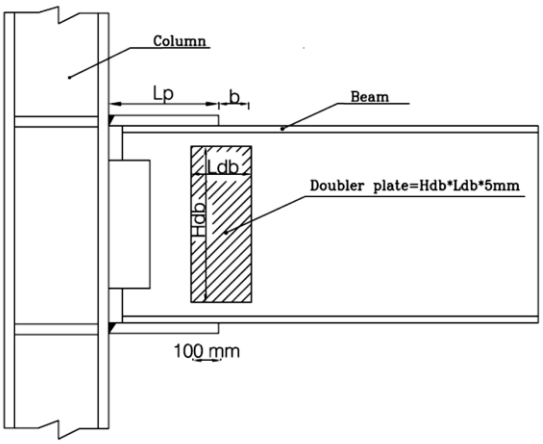

Figure 17. Strengthening of the beam web at the plastic hinge area using a doubler plate

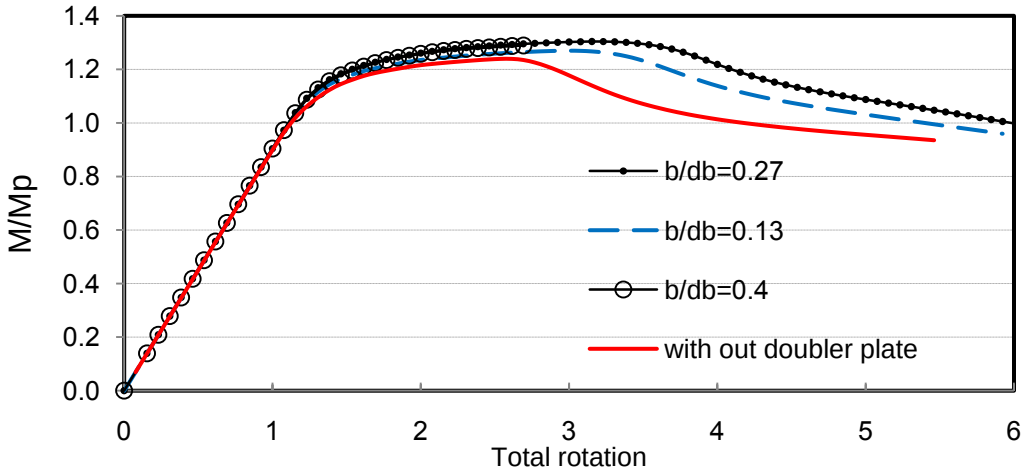

Figure 18. Moment-rotation curves of specimens RC06 with doubler plates of different size

Table 6: Results of WFP specimens with different sizes of the doubler plate

Specimen	H_{db}(mm)	L_{db}(mm)	t_{db}(mm)	b/d_b	M/Mp	θ(%)
RC06	-	-	-	-	0.71	5.5
	600	200	5	0.13	0.82	6
	600	300	5	0.27	0.86	6
	600	400	5	0.4	-	2.7
SPE07	-	-	-	-	0.81	5.46
	750	200	5	0.11	0.92	6
	750	300	5	0.22	-	3.07
SPE03	-	-	-	-	0.79	4.92
	400	200	5	0.16	0.82	6
	400	300	5	0.32	-	3

6. CONCLUSIONS

This study was aimed to investigate the effective parameters on the strength and ductility of the WFP connections with deep beams using the finite element method. The investigated parameters included, the material property of the beam, flange plate thickness, flange plate length, the transverse welding of the top flange plates, the form of the top flange plate, the equality or inequality of the top and bottom flange plate lengths and form of the rib plates. The conclusions drawn from this finite element study can be summarized as follows:

1. Decrease in the yield stress of the beam material delayed the initiation of the beam flange fracture at the plastic hinge region. This finally led to increase in the connection's strength, ductility and initial rotational stiffness. It also caused a reduction in the strength degradation of the connection after its yield point.
2. Similar to the other welded connections (e.g. pre or post-Northridge connections), the classic beam theory was invalid for the WFP connections. In other word, the flange plates considerably participated to transfer the shear force from the beam to the column. Consequently, It makes importance the selection of an appropriate method for transferring the shear forces from the beam to the column in order to reduce the tri-axially stresses at the flange plates at face of the column and to prevent the early fracture at this region.
3. The appropriate method to transfer the shear force from the beam to the column was a function of the L_P/d_b ratio. When L_P/d_b is more than o.6, generally using the rib plates was better than the use of the shear plate, whereas in L_P/d_b range which is less than 0.6, using the shear tab was the appropriate method.
4. Transverse welds which connect the noise of the top flange plate to the beam flange had no effect on the strength of the WFP connections. These welds caused a strain reduction across the beam flange at the noise of the top flange plate. However, this positive effect caused a strain concentration at the plastic hinge area and finally led to a slightly reduction in the connection ductility in compared to the one without transverse welds. Hence, it is recommended to use only the longitudinal welds for connecting the top flange plates to the beam flange. However, using the transverse welds can be effective to reduce the size of

fillet welds and consequently to decrease the thermal stresses at this area.

5. Generally the form of the top flange plate had no remarkable effect on the strength and ductility of the WFP connections. However, among all six forms, using the first, the second and the third forms led to the achievement of higher connection ductility with less strain concentration at the top flange plate at the column face level. Despite of the higher fabrication cost of the third form in compare to the second form, using the third form is recommended. Because in this case by rounding the intersection of the rectangular and the trapezoidal parts of the top flange plate, a remarkable reduction was achieved in the strain concentration at the SC point and consequently this reduces the probability of the fracture initiation at this critical point. In addition, using the fifth form of top flange plate led to the achievement of the minimum connection rotational capacity. However, it had no effect on the connection strength.
6. The best connection performance can be achieved when the length of the both top and bottom flange plates are equal.
7. By increasing the horizontal length of the rib plates the connection strength and ductility increased. Hence, in the case of using rib plates to transfer the shear forces from the beam to the column, the highest connection performance might be achieved when the flexural rib plates are used.
8. Considering all the recommendations presented in the above paragraphs, was significantly effective to increase the ductility of the WFP connections to achieve the minimum required ductility. However, the effects of these recommendations on the connection's strength enhancement were not pronounced.

Adding doubler plate at the beam web was effective to delay the beam web buckling and to increase the connection strength. The horizontal length of the doubler plate played a significant role on the connection ductility. Excessive increase in this parameter significantly reduced the connection ductility. Based on these limited results, the highest connection performance might be achieved when the b/d_b ratio of the doubler plate is limited to 0.13.

REFERENCES

1. Ramirez CM, Lignos DG, Miranda E, Kolios D. Fragility functions for pre-Northridge welded steel moment-resisting beam-to-column connections, *Engineering Structures*, **45**(2012) 574-84.
2. Mahin ST. Lessons from damage to steel buildings during the Northridge earthquake, *Engineering Structures*, **20**(1998) 261-70.
3. Miller DK. Lessons learned from the Northridge earthquake, *Engineering Structures*, **20**(1998) 249-60.
4. Engelhardt MD, Sabol TA. Reinforcing of steel moment connections with cover plates: benefits and modifications, *Engineering Structures*, **20**(1998) 510-20.
5. SAC. Experimental investigations of beam-column sub assemblages, Technical report SAC-96-01, parts 1 and 2. Sacramento, CA, SAC Joint Venture, (1996) 739-46.

6. Saffari H, Hedayat AA, Poorsadeghi Nejad M. Post-Northridge connections with slit dampers to enhance strength and ductility, *Journal of Constructional Steel Research*, **80**(2013) 138-52.
7. Popov EP, Yang TS, Chang SP. Design of steel MRF connections before and after 1994 Northridge, *Engineering Structures*, **20**(1998) 1030-38.
8. Hedayat AA, Celikag M. Post-Northridge connection with modified beam end configuration to enhance strength ductility, *Journal of Constructional Steel Research*, **64**(2009) 1413-30.
9. Hedayat AA, Celikag M. Wedge design: reduced beam web (RBW) connection for seismic regions, *Advances in Structural Engineering*, **13**(2010) 263-90.
10. Hedayat AA, Celikag M. Reduced beam web (RBW) connections with circular openings Structural Steel: Shapes and Standards, Properties and Applications**,** New York, USA, Nova Science Publishers Inc (2010) 1-56.
11. Hedayat AA, Saffari H, Mousavi M. Behavior of steel reduced beam web (RBW) connections with arch-shape cut, *Advances in Structural Engineering*, No. 10, **16**(2013) 1645-62
12. FEMA350 (2000), Recommended Seismic Design Criteria for New Steel Moment-Frame Buildings, Federal Emergency Management Agency, Washington, D.C.
13. Tsai KC, Popov EP. Seismic design of steel beam-to-box column connections, in *Proceedings of the Structures Congress '9*3, *ASCE*, (1993) 1226-31.
14. Popov EP, Jokerst M. Lawrence Berkeley National laboratory Human Genome Laboratory steel joint test: Technical brief. Forell/Elsesser Engineers, Inc, Unpublished report, July 20, 1995.
15. Whittaker AS, Gilani AS. Cyclic testing of steel beam-column connections, EERC-STI 1996/04. Berkeley, Calif: Earthquake engineering research center, University of California at Berkeley, 1995.
16. Noel A, Uang CM. Cyclic testing of steel moment connections for the San Francisco Civic Center Complex, TR-96/07. La jolla, Calif.: Structural System Research Project, University of California at San Diego, 1996.
17. SAC. Cover-Plate and Flange-Plate reinforced steel-moment resisting connections, Report No. SAC/BD-00/27, SAC Joint Venture, Sacramento, Calif, 2000.
18. Mansouri I, Saffari H. A new steel panel zone model including axial force for thin to thick column flanges, *Steel and Composite Structures*, No. 4, **16**(2014) 417-36.
19. Saffari H, Hedayat AA, Soltani Goharriz N. New alternatives for continuity plates in i-beam to box columns connections, *Asian Journal of Civil Engineering*, No. 4, **15**(2014) 547-61.
20. Mansouri I, Saffari H. New mathematical modeling of steel panel zone with thin to thick column flange, *Asian Journal of Civil Engineering (BHRC)*, No. 4, **16**(2015) 451-66.

21. Ghobadi MS, Mazroi A, Ghassemieh M. Cyclic response characteristics of retrofitted moment resisting connections, *Journal of Constructional Steel Research*, **65**(2009) 586-98.
22. Ghobadia MS, Ghassemiehb M, Mazroic M, Abolmaalid A. Seismic performance of ductile welded connections using T-stiffener, *Journal of Constructional Steel Research*, **65**(2009) 766-75.
23. Gholami M, Deylami A, Tehranizadeh M. Seismic performance of flange plate connections between steel beams and box columns, *Journal of Constructional Steel Research*, **84**(2013) 36-48.
24. FEMA355D, State of the art report on connection performance, Federal Emergency Management Agency, Washington, D.C, 2000.
25. ANSYS User Manual, ANSYS, Inc, 2010.
26. Gilton CS, Uang CM. Cyclic response and design recommendations of weak-axis reduced beam section moment connections, *Journal of Structural Engineering-ASCE*, No. 4, **128**(2002) 452-63.
27. Mao C, Ricles J, Lu L, Fisher J. Effect of local details on ductility of welded moment connections, *Journal of Structural Engineering, ASCE*, (2001) 1036-44.
28. Ricles JM, Mao C, Lu LW, Fisher JW. Ductile details for welded unreinforced moment connections subject to inelastic cyclic loading, *Engineering Structures*, **25**(2003) 667-80.
29. AISC, Seismic provisions for structural steel buildings, AISC/ANSI341–10, Chicago (IL), American Institute of Steel Construction, Inc, 2010.
30. AISC, Specification for Structural Steel Buildings, ANSI/AISC360-10, June 22, 2010.
31. Saffari H, Hedayat AA, Soltani GN. Suggesting double-web I-shaped columns for omitting continuity plates in a box-shaped column, *Steel and Composite Structures*, No. 6, **15**(2013) 585-603.
32. Berman JW, Okazaki T, Hauksdottir HO. Reduced link sections for improving the ductility of eccentrically braced frame link-to-column connections, *Journal of Structural Engineering*, No. 5, **136**(2009) 543-53.
33. Chao SH, Khandelwal K, El-Tawil S. Ductile web fracture initiation in steel shear links, *Journal of Structural Engineering, ASCE*, No. 8, **132**(2006) 1192-1200.
34. Prinz GS, Richards PW. Eccentrically braced frame links with reduced web sections, *Journal of Constructional Steel Research*, **65**(2009) 1971-8.
35. Lee KH, Stojadinovic B, Goel SC, Margarian AG, Choi J, Wongkaew A, Reyher BP, Lee DY. Parametric Tests on Unreinforced Connections, SAC/BD-00/01, Final Report, **I**(2000).
36. SAC, Experimental Investigations of Beam-Column Sub assemblages, Technical Report SAC-96-01, Parts 1 and 2, SAC Joint Venture, Sacramento, CA, 1996.
37. Iranian National Building code, part 10, 2008.
38. Cheol HL. Review of force transfer mechanism of welded steel moment connections, *Journal of Constructional Steel Research*, No. 7, **62**(2006) 695-705.